ELECTRONIC NATURE OF B–H–B BRIDGES AND THEIR MANIFESTATION IN VIBRATIONAL SPECTRA OF 11-VERTEX *nido*-CARBABORANES

Larissa A. LEITES[1,*], Elena G. KONONOVA and Sergey S. BUKALOV

A. N. Nesmeyanov Institute of Organoelement Compounds, Scientific and Technical Center on Raman Spectroscopy, Russian Academy of Sciences, 28 Vavilova Str., Moscow 119 991, Russia; e-mail: [1] buklei@ineos.ac.ru

Received August 31, 2007
Accepted October 25, 2007

AIM analysis of electron density function based on the results of DFT B3LYP calculations was carried out for six 11-vertex *nido*-carbaboranes containing B–H–B bridges. The vibrational modes of B–H–B bridges were investigated experimentally and theoretically. The results obtained allowed some conclusions about the electronic structure of the species studied and the role of B–H–B bridges in the cage bonding pattern.

Keywords: 11-Vertex *nido*-carbaboranes; B–H–B bridge; Electronic structure; Raman and IR spectroscopy; Density functional calculations; Molecular graph.

Electron-deficient polyhedral 11-vertex carbaboranes of the *nido* structural type with one[1–4], two, or three[5] carbons in the cage can contain the "extra" or "acid" or "facial" hydrogen atoms, which occupy mostly B–H–B bridging positions and evidently play an important role in molecular stabilization, completing the cage bonding system to $2(n+2)$ electrons, in accord with the Williams–Wade skeletal electron counting rules[6,7]. The polyhedral framework of these compounds with atom numbering is depicted in Fig. 1. Being precursors to many icosahedral metallacarbaboranes and *closo*-carbaboranes,

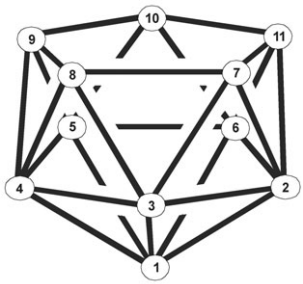

FIG. 1
11-Vertex *nido* polyhedron with the cage atom numbering

Collect. Czech. Chem. Commun. 2007, Vol. 72, No. 12, pp. 1659–1675

doi:10.1135/cccc20071659

these *nido* species play an important role in modern boron chemistry. The most common are *nido*-dicarbaboranes $\{C_2B_9\}$, their isomers with 7,8, 7,9 (ref.[8]), 2,7 (ref.[9]), 2,9 (refs[10–12]) and 2,8 (ref.[13]) positions of carbon atoms are reported.

Since their discovery in the 1960's[8a,8b], the 11-vertex *nido*-carbaboranes have been widely studied experimentally and theoretically; in recent years the group from Durham University has been very active in this field[4,12–14]. The experimental methods used are mainly X-ray analysis and NMR spectroscopy; the number of vibrational studies is scarce. Theoretical papers include geometry optimization, NMR and energy calculations. All the results show that the molecular properties noticeably depend on the number and location of the bridged hydrogen atoms H_b on the open face. The same was demonstrated on examples of 6-vertex *nido* species in ref.[15].

Analysis of the experimental and computed geometries of the 11-vertex *nido*-carbaboranes reveals wide dispersion in the values of interboron distances. Notably, the B–B distance under the hydrogen bridge is always longer compared with the B–B distances inside the cage. This fact, which was noticed by Wade[7a] and analyzed by Mitchell and Welch[16], is evidently related to a peculiar bonding pattern of such structures.

However, the methods applied have not been able to provide a "full-blown", complete insight into the role of the H_b atoms in the cage bonding. To partly eliminate this shortcoming, we present here the results of our study of some 11-vertex *nido* species by the Bader "Atoms in Molecules" (AIM) method[17], i.e., by theoretical topological analysis of the electron-density function. This approach has proven to be a successful tool in understanding the details of polyhedral borane and carbaborane structures[18–20]. As vibrational spectra always reflect distinctive features of electron bonding, it seems also useful to investigate experimentally and theoretically the effect and manifestation of the B–H–B bridges in vibrational (Raman and IR) spectra.

According to the number, location and geometry of the B–H–B bridges on the open face, the 11-vertex *nido*-carbaboranes can be divided into the following four types (Fig. 2):

I. Polyhedra with one symmetric B–H–B bridge ($[7,9\text{-}C_2B_9H_{12}]^-$ (**1**) and $7,8,9\text{-}C_3B_8H_{12}$ (**2**));

II. Polyhedra with one asymmetric B–H–B bridge ($[7,8\text{-}C_2B_9H_{12}]^-$ (**3**));

III. Polyhedra with two adjacent bridges ($7,8\text{-}C_2B_9H_{13}$ (**4**));

IV. Polyhedra with two non-adjacent bridges ($[7\text{-}CB_{10}H_{13}]^-$ (**5**) and $11\text{-Me-}2,7\text{-}C_2B_9H_{12}$ (**6**)).

The compounds of each type studied by us are indicated in brackets, they include species with one (**5**), two (**1**, **3**, **4**, **6**) and three (**2**) carbon atoms.

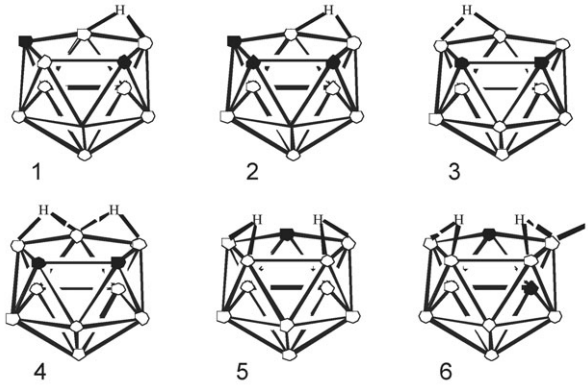

FIG. 2
The species studied

RESULTS AND DISCUSSION

AIM Analysis of Electron Density Distribution

The bonding patterns of the structures **1**–**6** were elucidated on the basis of theoretical topological analysis of the electron density (ED) function. As a result, the corresponding molecular graphs with their sets of critical points were determined and the values of electron density $\rho(\mathbf{r})$ at (3,+1) ring critical points (RCP) and (3,–1) bond critical points (BCP) were obtained. Some of these are presented in Table I and in Figs 3a–3c.

As it could be expected, the AIM results for the above listed *nido*-carbaboranes have much in common with those for *closo* clusters, investigated by this method earlier[18–20]. Namely, the bonding in the cage is realized via both multicenter bonds and two-center bonds with reduced order. The $\rho_r(\mathbf{r})$ values for most rings are shown not to differ significantly from the values of $\rho_b(\mathbf{r})$ for the intracage bonds. This is typical of electron-deficient polyhedral species and points to a substantial charge delocalization over the cage surface. It is also notable that, like *closo* clusters, the *nido* polyhedra studied exhibit in their interiors a critical point of the type (3,+3), which indicates the presence of a cage in spite of the fact that they possess an "open face". However, *nido* structures exhibit some interesting peculiarities compared with *closo* congeners.

In all types of the species studied, each *extra*-hydrogen atom H_b is linked to two boron atoms by two-center B–H_b bonds. The values of $\rho_b(\mathbf{r})$ at BCP(3,–1) for these bonds are similar for all types of the entities studied (Table I) and appeared to be comparable with those for the intracage B–B bonds (0.125–0.108 a.u.). As $\rho_b(\mathbf{r})$ values provide a measure of the bond order, these data mean that the *extra*-hydrogen atoms are equal participants in the cage bonding system. This finding is in good accord with Williams' statement that bridge hydrogens when present are of primary structural importance which should not be underrated[6b]. In the case of the symmetrical

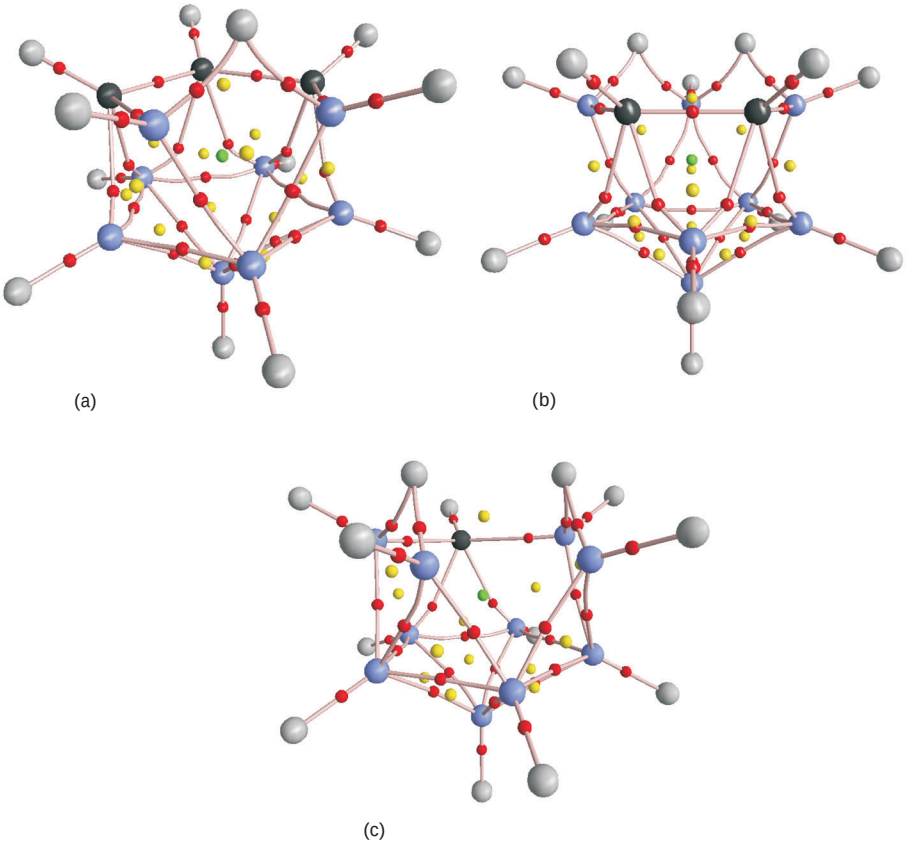

FIG. 3
Molecular graphs of (a) 7,8,9-$C_2B_9H_{12}$ (**2**), (b) 7,8-$C_2B_9H_{13}$ (**4**) and (c) $[CB_{10}H_{13}]^-$ (**5**). Ring, bond and cage critical points are indicated and denoted by small yellow, red and green circles, respectively

bridges, the $\rho_b(\mathbf{r})$ values are equal for both parts of the bridge, whereas for the asymmetrical ones they may be essentially different (see Table I where corresponding B–H_b distances are also presented for comparison).

Another interesting feature, common to all the molecular graphs obtained, is that the boron atoms involved in the B–H–B bridge are not linked by the lines of the maximum charge density, i.e., there is no two-center edge-localized bond between them; they are held together only by multicenter bonding. Here is the reason for lengthening of the corresponding B–B distances (>1.85 Å) noted previously. It should be pointed out that this result, i.e. the absence of bond critical points between the boron atoms participating in the B–H–B bridge, was first obtained by Bader and Legar[18a] for small *nido*-B_5H_9 and *arachno*-B_6H_{10} boranes.

Due to this peculiarity, the "open faces" of the 11-vertex *nido* clusters are effectively not pentagonal, as it is commonly accepted, but of larger size, since they involve not only C and B atoms, but also H_b atoms. This leads to the formation of a six-membered ring in the *nido* structures of **1** and **2** with their single B–H–B bridge. This is illustrated by a molecular graph for anion **2** in Fig. 3a. Experimental geometries of anion **1** and its derivatives can be found in refs[14a,21,22], of molecule **2** in ref.[5b]

TABLE I
The B–H_b distances *d* and electron densities $\rho_b(\mathbf{r})$ at (3,–1) B–H_b bond critical points in the B–H–B bridges of some 11-vertex *nido*-carbaboranes

Polyhedron	Bond	*d*(B–H), Å[a]	$\rho_b(\mathbf{r})$, a.u.
7,8,9-$C_3B_8H_{12}$	B10–H_b = B11–H_b	1.312[5b,5c]	0.124
[7,9-$C_2B_9H_{12}$]$^-$	B10–H_b = B11–H_b	1.23[14a]	0.124
[7,8-$C_2B_9H_{12}$]$^-$	B10–H_b	1.252	0.132
	B11–H_b	1.469[14c]	0.113
7,8-$C_2B_9H_{13}$	B9–H_{b1} = B11–H_{b2}	1.27	0.127
	B10–H_{b1} = B10–H_{b2}	1.35	0.114
[7-$CB_{10}H_{13}$]$^-$	B8–H_{b1} = B11–H_{b2}	1.33	0.112
	B9–H_{b1} = B10–H_{b2}	1.22[3]	0.130
11-CH_3-2,7-$C_2B_9H_{12}$	B8–H_{b1}	1.32 (1.35)	0.119
	B9–H_{b1}	1.21 (1.19)	0.127
	B10–H_{b2}	1.03 (1.17)	0.137
	B11–H_{b2}	1.50[9b] (1.39)	0.117

[a] X-ray data for 11-Ph-CH_2-2,7-$C_2B_9H_{12}$ are given in parentheses.

Similarly, there is a seven-membered ring in the molecular graph of the species **4** with its two adjacent asymmetric B–H–B bridges[8,13,14a] (Fig. 3b). These larger rings exhibit lowered $\rho_r(\mathbf{r})$ values at their (3,+1) ring critical points – 0.028 a.u. The absence of the above mentioned edge-localized B–B bonds also results in the formation of four-membered rings in the cage below the B–H–B bridges, but this does not cause a notable weakening of the multicenter bonding in the corresponding parts of the polyhedra, since the values of $\rho_r(\mathbf{r})$ for four-membered rings (0.105–0.090 a.u.) are only slightly lower than those for ordinary triangular faces (~0.110 a.u.).

The molecular graphs obtained for the *nido* species **5** and **6** (type **IV**), having two non-adjacent asymmetric B–H–B bridges, appeared especially interesting. Geometry data for the polyhedra with a single carbon atom in the open face (such as species **5**, **6**, as well as 2,8-$C_2B_9H_{13}$ and 2,9-$C_2B_9H_{13}$ (refs[2–4,9b,12,13,14a])) show that the B–B distance between the bridges (~1.91 Å) is even longer than those under the bridges. The rationale for this fact was also found in the results of AIM calculations. They demonstrate that, in addition to the absence of the two-center bonds under the B–H–B bridges, there is no (3,–1) bond critical point between the atoms B9 and B10, so the bridges are not connected directly by an edge-localized B–B bond. Consequently, the formally five-membered open faces of species **5** and **6** are even larger than in **1**–**4**, as they encompass 8 atoms (see, i.e., the molecular graph of anion **5** in Fig. 3c). The corresponding value of $\rho_r(\mathbf{r})$ for this eight-membered ring is very low (~0.020 a.u.). Thus, not only the two-center bond between the B9 and B10 atoms in **5** and **6** is missing, but also the multicenter bonding between them is weaker compared with that of other parts of the cage. The essential $\rho_r(\mathbf{r})$ drop at RCPs of the six-membered and larger-size rings results in uneven distribution of "electronic glue"[18a] over the surface of these polyhedra.

A comparison of the results for species **3** and **4** allowed us to make some conclusions concerning the influence of the number of H_b atoms on the electronic structure of 7,8-dicarba-*nido*-polyhedron. First, appearance of an additional H_b atom causes a slight decrease in the $\rho_b(\mathbf{r})$ values of the two-center B–B bonds (0.126–0.109 a.u. in **3** and 0.120–0.105 a.u. in **4**) and C–B bonds (0.151–0.121 a.u. in **3** and 0.143–0.125 a.u. in **4**) and in $\rho_r(\mathbf{r})$ values of the corresponding rings (0.117–0.105 a.u. in **3** and 0.117–0.092 a.u. in **4**). This indicates some weakening of both two-center and multicenter bonding and explains a certain elongation of interatomic distances in polyhedron **4** compared with **3** and a lower stability of the former. Second, the presence of the second H_b atom leads to a noticeable rise in $\rho_b(\mathbf{r})$ magnitudes for terminal B–H and C–H bonds (0.181–0.186 a.u. and 0.283 a.u. in

molecule **4** compared to 0.174–0.170 a.u. and 0.278 a.u. in anion **3**, respectively).

Thus the data obtained clearly demonstrate a considerable effect of the location of B–H–B bridges and of their number on the electronic structure of the 11-vertex *nido* polyhedra.

Vibrational Spectra

Already Hawthorne et al.[8] observed weak bands in the region 1600–2000 cm^{-1} of the IR spectrum of anion **1** and molecule **4** and assigned them to vibrational modes with *extra*-hydrogen atom participation. This assignment was confirmed by the IR results for μ-deuterated species. Afterwards two of us succeeded in detecting the *extra*-hydrogen vibrations in the Raman spectra of *nido* species **1**, **3**, **6** and their derivatives[23] as weak broad polarized features in the region 1700–2350 cm^{-1}. Deuteration of the *extra*-hydrogen atoms shifted these features to the region 1300–1650 cm^{-1} with a normal isotopic ratio of ~1.3. As this spectral interval was shown to be typical of B–H–B bridges in the spectra of boranes[24,25] and also of a small *nido*-carbaborane[26], an inference was drawn that the *extra*-hydrogen atoms also form B–H–B bridges on the open faces of the *nido* polyhedra studied. In 1992 all vibrational results were reviewed in ref.[27]. Later on, we reported full Raman and IR spectra of **5** [28], now the investigations are being extended to cover the spectra of **2** and **4** [29].

However, the normal coordinate calculations for the *nido* species have not been carried out, and therefore systematic comparative analysis of the B–H–B bridge vibrational modes was not possible. In this paper, we discuss the vibrational spectra of **1**–**6**, in particular those in the region 1500–2300 cm^{-1}, based on our Raman and IR experiments published in refs[23,27] and renewed[28,29], and also on the results of normal coordinate analysis (NCA). The normal mode frequencies, IR intensities and eigenvectors were calculated at the B3LYP/6-311++G(d,p) level. The computations, being carried out in a harmonic approximation, correctly reproduce the mode frequencies in the middle region of the spectra, but, as expected, overestimate the frequencies in the region 1800–3100 cm^{-1}, corresponding to stretching vibrations of bonds with hydrogen atom participation. These are the well-localized ν/δBHB (see below), νBH_t and νCH modes. All the other normal modes are shown to be of heavily mixed origin.

The species studied (molecules **2**, **4**, **6** and isolated anions **1**, **3**, **5**) belong either to the C_s (**1**, **2**, **4**, **5**) or to C_1 (**3**, **6**) point symmetry group; thus, all their normal modes should be active in the Raman and IR spectra.

Let us analyze the vibrational modes, involving displacements of the *extra*-hydrogen atom. One B–H–B grouping possesses three vibrational degrees of freedom. Normal coordinate analysis for the species of the type **I** with one symmetric B–H–B bridge predicts two well-localized normal modes with frequencies of ~1980 and ~1700 cm^{-1}. Animation of mode eigenvectors reveals that the first mode (observed as a weak structured Raman and IR feature at about 1900 cm^{-1}) is a movement of the H_b atom parallel to the coordinate axis *z* (Fig. 4). This displacement is a symmetric stretch of both B–H_b bonds but it inevitably leads to a simultaneous change in the BHB angle; thus, we designate it as a ν/δ mode of the A′ type. On deuteration of the H_b atom (μ-deuteration), its experimental frequency moves to ~1450 cm^{-1} with a normal νBH/νBD ratio of ~1.3. The second mode is the displacement of the H_b atom strictly parallel to the coordinate axis *x* and antisymmetric with respect to the mirror plane. Its calculated IR intensity is zero; indeed, this mode manifests itself in the spectra as a very weak broad feature, hardly detectable in the region 1700–1800 cm^{-1}, but notably moving down on μ-deuteration to ~1380 cm^{-1} (νBH/νBD ratio ~1.3). This mode is an analog of the antisymmetric stretch of the B–H_b bonds but it also involves deformation of the BHB angle. Thus, it is a ν/δBHB mode of the A″ type. The interval of these BHB mode frequencies agrees with that of the $\rho_b(\mathbf{r})$ values at (3,–1) BCPs for the B–H_b bonds in the bridge (Table I). Both these sets of values are comparable with those for the intracage bonds but are lower than those for terminal B–H_t bonds. The absence of the edge-localized B–B bond under the B–H–B bridge, which follows from the AIM results (see Fig. 3a) and manifests itself in lengthen-

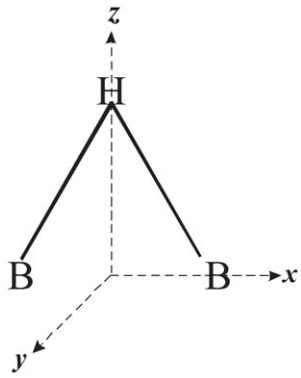

FIG. 4
Coordinate axes for a B–H–B bridge

ing of the corresponding B–B distance, is also reflected by the vibrational spectra, giving rise to peculiar normal modes in the region below 600 cm^{-1} with predominant participation of the ν(B10–B11) stretching coordinate, i.e., including movements of the "loose" boron atoms.

The results of NCA show that the third B–H–B vibration is the displacement of the H_b atom parallel to the coordinate axis *y*. It is not localized, being heavily mixed with other vibrational coordinates and taking part in several normal modes of the A′ type with frequencies lower than 1150 cm^{-1}. These can be identified by a notable (up to 50 cm^{-1}) downshift of their frequencies in the spectra of μ-deuterated compounds. It is noteworthy that such a strong vibrational coupling is possible only if the force constants of $B–H_b$ bonds are comparable with those of the intracage ones – the idea consistent again with the results of the topological analysis of ED.

Two B–H–B groupings in a polyhedron should formally generate six normal modes. For the polyhedra **4**, **5**, **6**, NCA results predict three of them to be well-localized, whereas the fourth lowest-frequency one is mixed with δBH_t vibration. These modes are in-phase and out-of-phase combinations of the two ν/δ modes described above for the structures of the type **I**. The remaining modes, involving displacements of the H_b atoms parallel to coordinate axis *y*, are again heavily mixed with other vibrational coordinates.

For the case of two adjacent asymmetric bridges (type **III**, molecule **4** of point group C_s, its optimized geometry with elongated B–B distances under the bridges is reported in ref.[12]), the calculated frequencies and mode descriptions are shown below in Fig. 5.

In the experimental spectrum of molecule **4**, only two broad, weak, structured features in the region 1980–2100 cm^{-1} and at ~1520 cm^{-1} are observed in both IR and Raman spectra. Each of these features evidently incorporates both in-phase and out-of-phase modes with mainly vertical and mainly horizontal displacements of the H_b atoms, respectively, as well as several non-fundamentals (see below). Quite an analogous B–H–B spec-

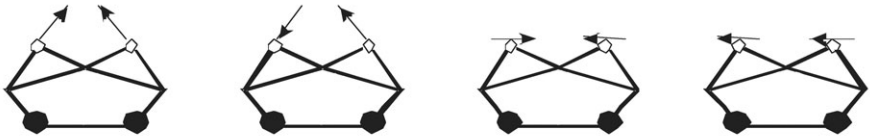

FIG. 5
Calculated frequencies and mode description for two adjacent B–H–B bridges

tral pattern was reported for a small *nido*-carbaborane, 4,5-$C_2B_4H_8$, which has the same structure of the open face[26].

Anion **5** and molecule **6** (Fig. 2) with two non-adjacent asymmetric bridges belong to type **IV**. NCA performed for monocarbaborane **5** of C_s symmetry resulted in the following calculated frequencies of the ν/δBH_bB modes (Fig. 6).

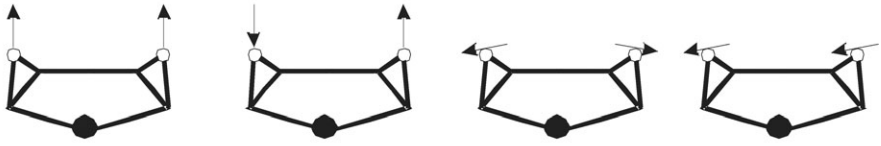

FIG. 6
Calculated frequencies and mode description for two non-adjacent B–H–B bridges

The first two modes again involve mostly vertical while the last two modes mostly horizontal H_b atom displacements. In the experimental spectrum of anion **5**, the following features correspond to these predictions: ~2025 cm^{-1} (R, IR, medium intensity), ~1850 cm^{-1} (IR, weak), ~1450 cm^{-1} (R, weak) and ~1380 cm^{-1} (IR, weak). Quite a different pattern in this region was observed for another *nido* species of the type **IV**, but containing two carbon atoms and a methyl group, namely, 11-methyl-2,7-dicarba-*nido*-undecaborane (**6**). Introduction into the cage of the second carbon atom in position 2 and B–Me-substitution results in a significant increase in the frequencies of the B–H–B bands. The whole feature involving these bands extends from 1700 to 2300 cm^{-1}. On deuteration of both H_b atoms, this feature disappears completely and a system of bands in the region 1450–1650 cm^{-1} appears instead (Fig. 7).

It is necessary, at last, to draw attention to an unusual spectral pattern in the region 1700–2300 cm^{-1}, which was first noticed for **1** and its derivatives in refs[23,27]. Such a pattern, complicated in both Raman and IR spectra, exhibiting broad bands with a fine structure with many small peaks, was observed for all the compounds studied, except for anion **3** and its derivatives. Typical examples are given in Figs 7 and 8. This fine structure cannot be explained by crystal effects because it is preserved in the spectra of solutions. Analysis of literature data shows that such spectral pattern is characteristic of all B–H–B bridges and is explained by Fermi resonance, caused by inter-

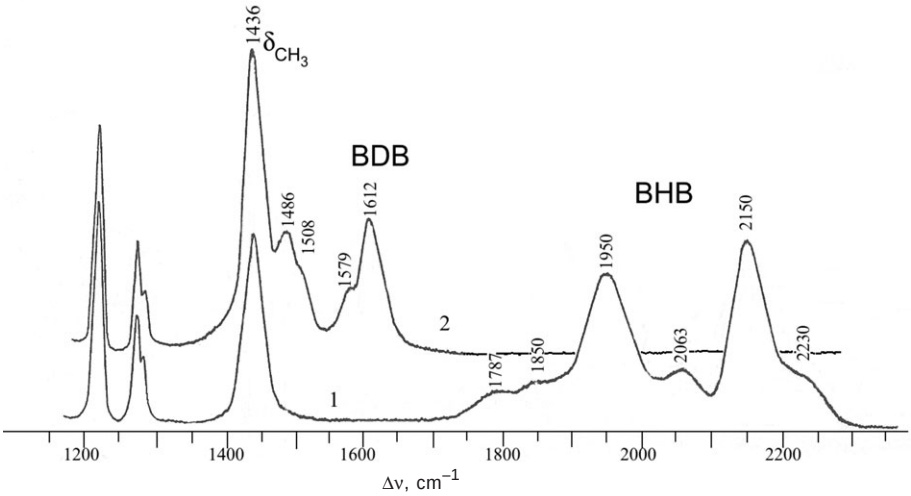

FIG. 7
The regions of BHB and BDB vibrations in the Raman spectra of solid 11-Me-2,7-$C_2B_9H_{12}$ (*1*) and its μ-d_2 derivative (*2*)

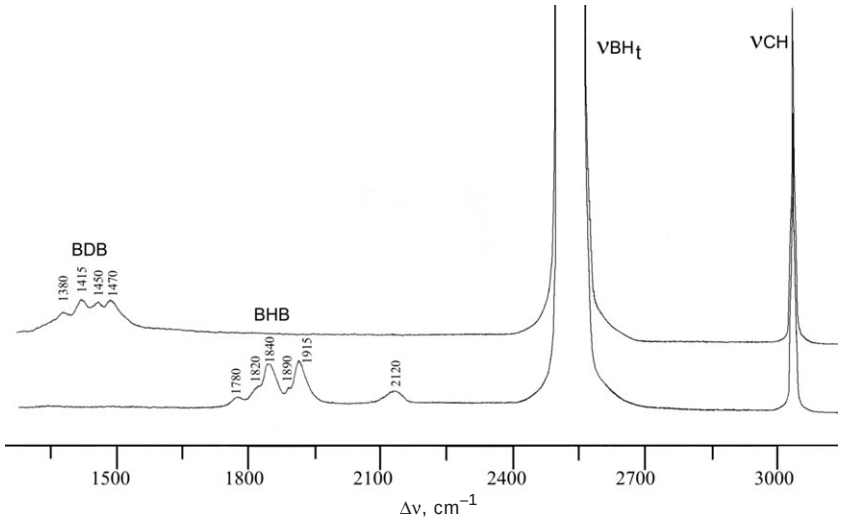

FIG. 8
The regions of BHB and BDB vibrations in the Raman spectra of solid Cs[7,9-$C_2B_9H_{12}$] and its μ-*d* derivative. The νBH_t and νCH regions are presented for intensity comparison

action between fundamental vibrational levels and overtone and/or combination levels of the same symmetry species. A detailed discussion of this phenomenon on the example of methyldiborane vibrational spectra can be found in ref.[24]. Bearing this in mind, weak broad Raman bands in the region 2100–2220 cm^{-1} in the spectra of **1** (Fig. 8) and **2** can be interpreted as overtones and combinations of the normal modes situated in the region 1050–1120 cm^{-1}, which are of mixed origin but with significant H_b atom participation. These overtones and combination bands acquire appreciable intensity because of extensive Fermi resonance with the totally symmetric fundamental. Since Fermi resonance leads to a noticeable perturbation of energy levels, it is not surprising that the observed intervals between the BHB mode frequencies do not correspond to the calculated ones.

The problem of spectral manifestations of B–H–B bridges is interesting and not clear yet. Possible band splittings due to boron isotopes should not be neglected hereby. However, the main peculiarities of the ν/δ(BHB) bands, i.e., their broadening and Fermi-resonance fine structure, seem to be characteristic of all vibrational bands associated with the stretching modes of doubly coordinated hydrogen atom. For instance, M–H–B bridges[30,31] and hydrogen bonds of the type A–H···B [32] exhibit analogous spectral patterns.

Quite apart is the anion **3**, for which the NCA calculation predicts only one well-localized ν/δBHB vibration at about 2170 cm^{-1} which involves the vertical H_b atom displacement (Fig. 4). The horizontal displacement of the H_b atom is strongly mixed with the deformational vibration of the B10–H_t bond, generating a mode with a frequency at ~1380 cm^{-1}. Indeed, for all the salts and derivatives of anion **3**, a single feature is observed at about 2100 cm^{-1} in the Raman spectrum, but not in IR. It is replaced by that at ~1550 cm^{-1} on μ-deuteration (Fig. 9). In contrast to the spectra of **1**, **2**, **4**–**6**, this feature is not only very broad but also symmetric and "smooth". It is known that location of the *extra*-hydrogen atom in the solid salts of anion **3** has remained contentious for many years after the discovery of these compounds and many differing X-ray results were published for various salts of **3** and its derivatives[14b,33–38]. A recent (2001) precise neutron diffraction study performed at 30 K for the salt $[PSH]^+[nido\text{-}7,8\text{-}C_2B_9H_{12}]^-$ by Fox et al.[14c] clearly localized this hydrogen atom as an asymmetric B–H–B bridge over the elongated B10–B11 edge, with B–H_b distances B10–H12 –1.252(10) Å and B11–H12 –1.469(11) Å. However, calculations carried out for isolated anion **3** at different levels of theory showed that the energy difference between the structures varying in H_b atom position is very small. The authors[14c] noted that the results cited above do not rule out the possibility of other geometries in another solid-state environment.

We believe that the special B–H–B band contour observed in the Raman spectra of the salts and derivatives of anion **3** is a consequence of the dynamic migration of the *extra*-hydrogen atom between the equivalent B9–H–B10 and B10–H–B11 positions, which is fast on the time scale of vibrational spectroscopy. This migration increases the effective symmetry of anion **3** from C_1 to C_s and makes the displacement of the H_b atom antisymmetric with respect to the mirror plane, thus preventing this mode interaction with symmetric overtones and combinations. As a result, the band becomes very broad (with a half-width ~85 cm^{-1} at room temperature and ~50 cm^{-1} at 30 K) and exhibits no Fermi-resonance structure. Numerous NMR data have established that anion **3** is fluxional in solution (see, i.e., a quite recent study of this problem by using ab initio/GIAO approach[39]). A vibrational evidence of H_b atom flipping, leading to the effective C_s symmetry of the cage **3**, is the presence in the solution-state Raman spectrum of anion **3** of polarized and depolarized components in the wide feature at ~2600 cm^{-1}, corresponding to νBH_t vibrations. The fact that the ~2100 cm^{-1} band contour in the Raman spectra of solid salts of anion **3** is quite similar to that of solutions (Fig. 9) is very important. It allows a conclusion that

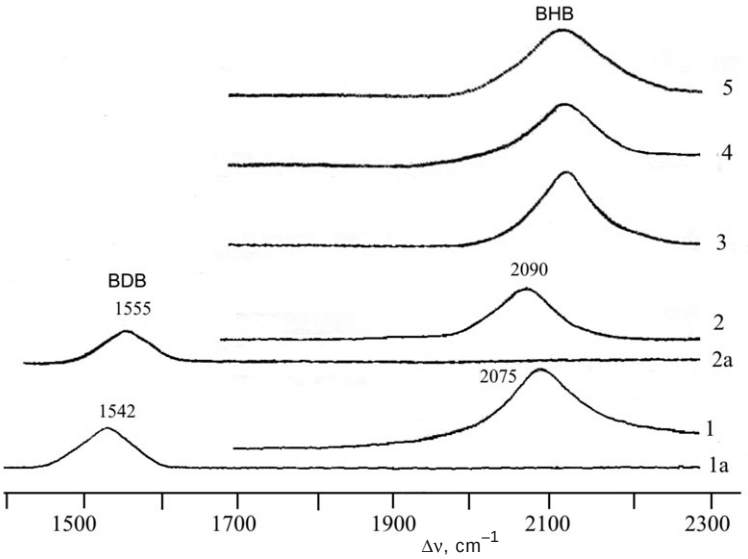

FIG. 9

The regions of BHB and BDB vibrations in the Raman spectra of various salts of $[7,8\text{-}C_2B_9H_{12}]^-$ and their μ-*d* derivatives. Solid Cs^+ salt (1) and its μ-*d* derivative (1a), solid zwitterion 6(5)-Me_2SO-7,8-$C_2B_9H_{11}$ (2) and its μ-*d* derivative (2a), solid NMe_4^+ salt (3), solid K^+ salt (4), aqueous solution of Cs^+ salt (5)

the dynamics mentioned above takes place in the crystalline state as well. The difference between the results of neutron diffraction and Raman spectroscopy could be explained by different time scales of the two methods.

One more interesting feature of vibrational spectra of the *nido* structures studied is a notable dependence of the νBH_t frequencies on the number of the H_b atoms. The presence of an additional H_b atom in molecule **4** compared with anion **3** causes a rise in the averaged νBH_t frequency value from ~2550 to ~2600 cm^{-1}. The latter value is typical of dicarba-*closo*-boranes $C_2B_{10}H_{12}$ (ref.[27]). The same is observed for monocarbaboranes; namely, the averaged νBH_t frequency values of the monocarba-*closo*-borane $[CB_{11}H_{12}]^-$ (ref.[28]) and of the *nido* anion **5** with its two H_b atoms are similar (~2550 cm^{-1}). These data are also in a good accord with the results of topological analysis of ED.

EXPERIMENTAL

The compounds studied were synthesized according to known methods: **1**, **3**, **4** (ref.[8]); **2** (ref.[5]); **5** (ref.[40]); **6** (ref.[9]).

The Raman spectra of **1**–**6** as well as of their μ-deuterated analogs in the region 100–3700 cm^{-1} were registered using Jobin–Yvon Ramanor-HG2S and LabRAM-300 spectrometers. The laser source used was either Ar^+ at 488.0 nm or He–Ne at 632.8 nm. Depolarization ratios of the Raman lines in the spectra of the aqueous solutions of the studied salts were estimated qualitatively. IR spectra in the region 200–3500 cm^{-1} were recorded in polyethylene and KBr pellets, as well as in Nujol mulls, using a M-82 Carl Zeiss spectrophotometer and a Nicolet Magna-750 FTIR spectrometer.

Geometry optimization and calculations of the vibrational mode frequencies, IR intensities and eigenvectors for isolated anions **1**, **3**, **5** and molecules **2**, **4**, **6** were carried out at the DFT B3LYP/6-311++G(d,p) level, using the G94W program suite[41]. Topological analysis of the theoretical electron density distribution (based on the results of the DFT calculation) was accomplished using the AIMpac program package[42].

CONCLUSIONS

The results of topological analysis of the electron density function for 11-vertex *nido*-carbaboranes are consistent with the data of the vibrational spectroscopy. The values of electron density at B–H_b bond critical points and of ν/δBHB vibrational frequencies demonstrate that the bridging H_b atom is an equal participant in formation of the cage bonding system. The presence of a B–H–B bridge on the open face of the *nido* polyhedron leads to the absence of the edge-localized two-center B–B bond under the bridge, resulting in lengthening of the corresponding interboron distance. The presence of two non-adjacent B–H–B bridges results in a further weakening of bonding between the boron atoms of the open face due to the absence of

the two-center B–B bond between the two bridges and to weakening of the multicenter bonding in this part of the polyhedron. The size of the "open face" formed, involving not only C and B atoms, but also H_b atoms, depends both on the number and location of the B–H–B bridges.

The B–H–B vibrational modes of *nido* polyhedra with one symmetric bridge, as well as of those with two adjacent and two non-adjacent asymmetric bridges generate a complicated pattern in the region 1500–2200 cm^{-1} of the Raman and IR spectra, with broad weak features exhibiting fine structure. This pattern is explained by extensive Fermi resonance of the totally symmetric ν/δBHB fundamental with overtones and combinations of mixed normal modes with participation of the H_b atom displacements. In contrast, the single asymmetric B–H–B bridge in the solid salts of the anion $[7,8\text{-}C_2B_9H_{12}]^-$ manifests itself only in the Raman spectrum as a specific, very broad band of symmetrical contour, not exhibiting the Fermi-resonance structure. This fact allows an inference that the dynamic migration of the H_b atom of anion **3** between the two equivalent B–H–B positions takes place not only in solution but also in the solid state and is fast on the time scale of vibrational spectroscopy.

The results obtained clearly demonstrate that the number and location of the H_b atoms notably influence the electronic structure of the 11-vertex *nido*-carbaboranes.

The authors are greatly indebted to V. N. Kalinin, V. A. Olshevskaya, S. P. Knyazev, V. V. Grushin and D. S. Perekalin for supplying the samples of the compounds studied and also acknowledge partial financial support from the Russian Academy of Sciences in the framework of the program Theoretical and Experimental Study of Chemical Bonding (grant No. 591-07).

REFERENCES

1. Hyatt D. E., Owen D. A., Todd L. J.: *Inorg. Chem.* **1966**, *5*, 1749.
2. Whitaker C. R., Romerosa A., Teixidor F., Rius J.: *Acta Crystallogr., Sect. C: Cryst. Struct. Commun.* **1995**, *51*, 188.
3. Jeffery J. C., Jelliss P. A., Lebedev V., Stone F. G. A.: *J. Chem. Soc., Dalton Trans.* **1997**, 1219.
4. Batsanov A. S., Fox M. A., Goeta A. E., Howard J. A. K., Hughes A. K., Malget J. M.: *J. Chem. Soc., Dalton Trans.* **2002**, 2624.
5. a) Štíbr B., Holub J., Teixidor F., Viñas C.: *J. Chem. Soc., Chem. Commun.* **1995**, 795; b) Holub J., Štíbr B., Hnyk D., Fusek J., Císařová I., Teixidor F., Viñas C., Plzák Z., Schleyer P. v. R.: *J. Am. Chem. Soc.* **1997**, *119*, 7750; c) Bakardjiev M., Holub J., Hnyk D., Císařová I., Londesborough M. G. S., Perekalin D. S., Štíbr B.: *Angew. Chem. Int. Ed.* **2005**, *44*, 6222.

6. a) Williams R. E.: *Inorg. Chem.* **1971**, *10*, 210; b) Williams R. E.: *Adv. Inorg. Chem. Radiochem.* **1976**, *18*, 67; c) Williams R. E.: *Chem. Rev.* **1992**, *92*, 177; d) Williams R. E., Bausch J. W. in: *Boron Chemistry at the Beginning of the 21st Century* (Yu. N. Bubnov, Ed.), pp. 3–16. Editorial URSS, Moscow 2003.
7. a) Wade K.: *Adv. Inorg. Chem. Radiochem.* **1976**, *18*, 1; b) Fox M. A., Wade K. in: *Boron Chemistry at the Beginning of the 21st Century* (Yu. N. Bubnov, Ed.), pp. 17–26. Editorial URSS, Moscow 2003.
8. a) Wiesboeck R. A., Hawthorne M. F.: *J. Am. Chem. Soc.* **1964**, *86*, 1642; b) Hawthorne M. F., Young D. C., Garrett P. M., Owen D. A., Schwerin S. G., Tebbe F. N., Wegner P. A.: *J. Am. Chem. Soc.* **1968**, *90*, 862; c) Howe D. V., Jones C. J., Wiersema R. J., Hawthorne M. F.: *Inorg. Chem.* **1971**, *10*, 2516.
9. a) Knyazev S. P., Brattsev V. A., Stanko V. I.: *Doklady* **1977**, *234*, 299; b) Knyazev S. P., Brattsev V. A., Stanko V. I.: *Doklady* **1977**, 234, 323; c) Struchkov Yu. T., Antipin M. Yu., Brattsev V. A., Kirilova N. I., Knyazev S. P.: *J. Organomet. Chem.* **1977**, *141*, 133.
10. Plešek J., Heřmánek S.: *Chem. Ind. London* **1973**, 38.
11. Hawthorne M. F., Busby D. C.: *Inorg. Chem.* **1982**, *21*, 4104.
12. Mackie I. D., Robertson H. E., Rankin D. W. H., Fox M. A., Malget J. M.: *Inorg. Chem.* **2004**, *43*, 5387.
13. Fox M. A., Hughes A. K., Malget J. M.: *J. Chem. Soc., Dalton Trans.* **2002**, 3505.
14. a) Fox M. A., Goeta A. E., Hughes A. K., Johnson A. L.: *J. Chem. Soc., Dalton Trans.* **2002**, 2132; b) Davidson M. G., Fox M. A., Hibbert T. G., Howard J. A. K., Mackinnon A., Neretin I. S., Wade K.: *Chem. Commun.* **1999**, 1649; c) Fox M. A., Goeta A. E., Howard J. A. K., Hughes A. K., Johnson A. L., Keen D. A., Wade K., Wilson C. C.: *Inorg. Chem.* **2001**, *40*, 173; d) Fox M. A., Howard J. A. K., Hughes A. K., Malget J. M., Yufit D. S.: *J. Chem. Soc., Dalton Trans.* **2001**, 2263; e) Fox M. A., Hughes A. K., Johnson A. L., Paterson M. A. J.: *J. Chem. Soc., Dalton Trans.* **2002**, 2009.
15. Hofmann M., Fox M. A., Greatrex R., Schleyer P. v. R., Williams R. E.: *Inorg. Chem.* **2001**, *40*, 1790.
16. Mitchell G. F., Welch A. J.: *J. Chem. Soc., Dalton Trans.* **1987**, 1017.
17. Bader R. F. W.: *Atoms in Molecules: A Quantum Theory*, 438 pp. Clarendon Press, Oxford, U.K. 1990.
18. a) Bader R. F. W., Legare D. A.: *Can. J. Chem.* **1992**, *70*, 657; b) Keith T. A., Bader R. F. W., Aray Y.: *Int. J. Quantum Chem.* **1996**, *57*, 183.
19. a) Antipin M. Yu., Polyakov A. V., Tsirelson V. G., Kappkhan M., Grushin V. V., Struchkov Yu. T.: *Organomet. Chem. U.S.S.R.* **1990**, *3*, 421; b) Antipin M., Boese R., Blaser D., Maulitz A.: *J. Am. Chem. Soc.* **1997**, *119*, 326; c) Lyssenko K. A., Antipin M. Yu., Lebedev V. N.: *Inorg. Chem.* **1998**, *37*, 5834; d) Lyssenko K. A., Golovanov D. G., Mesheryakov V. I., Kudinov A. R.: *Russ. Chem. Bull.* **2005**, *54*, 911; e) Glukhov I. V., Lyssenko K. A., Korlyukov A. A., Antipin M. Yu.: *Russ. Chem. Bull.* **2005**, *54*, 547.
20. a) Kononova E. G., Leites L. A., Bukalov S. S., Zabula A. V., Pisareva I. V., Konoplev V. E., Chizhevsky I. T.: *Chem. Phys. Lett.* **2004**, *390*, 279; b) Kononova E. G., Leites L. A., Bukalov S. S., Pisareva I. V., Chizhevsky I. T.: *J. Mol. Struct.* **2006**, *794*, 148.
21. Subrtová V., Novák C., Línek A., Hasek J.: *Acta Crystallogr., Sect. C: Cryst. Struct. Commun.* **1984**, *40*, 1955.
22. Welch A. J., Weller A. S.: *J. Chem. Soc., Dalton Trans.* **1997**, 1205.
23. a) Leites L. A., Bukalov S. S., Vinogradova L. E., Kalinin V. N., Kobelkova N. I., Zakharkin L. I.: *Bull. Akad. Sci. U.S.S.R., Div. Chem. Sci.* **1984**, 880; b) Leites L. A., Bukalov S. S.,

Vinogradova L. E., Knyazev S. P., Strelenko Yu. A.: *Bull. Akad. Sci. U.S.S.R., Div. Chem. Sci.* **1986**, 1633; c) Leites L. A., Bukalov S. S., Grushin V. V.: *Bull. Akad. Sci. U.S.S.R., Div. Chem. Sci.* **1989**, 2424; d) Leites L. A., Kats G. A., Bukalov S. S., Komarova L. G.: *Bull. Akad. Sci. U.S.S.R., Div. Chem. Sci.* **1991**, 316.

24. a) Carpenter J. H., Jones W. J., Jotham R. W., Long L. H.: *Spectrochim. Acta, Part A* **1970**, *26*, 1199; b) Carpenter J. H., Jones W. J., Jotham R. W., Long L. H.: *Spectrochim. Acta, Part A* **1971**, *27*, 1721.
25. a) Hanousek F., Štíbr B., Heřmánek S., Plešek J.: *Collect. Czech. Chem. Commun.* **1972**, *37*, 3001; b) Hanousek F., Štíbr B., Heřmánek S., Plešek J.: *Collect. Czech. Chem. Commun.* **1973**, *38*, 1312.
26. Jotham R. W., McAvoy J. S., Reynolds D. J.: *J. Chem. Soc., Dalton Trans.* **1972**, 473.
27. Leites L. A.: *Chem. Rev.* **1992**, *92*, 279.
28. Kononova E. G., Bukalov S. S., Leites L. A., Lyssenko K. A., Olshevskaya V. A.: *Russ. Chem. Bull.* **2003**, *52*, 85.
29. Leites L. A., Kononova E. G., Bukalov S. S., Aysin R. R., Perekalin D. S., Kalinin V. N.: Unpublished results.
30. Marks T. J., Kolb J. R.: *Chem. Rev.* **1977**, *77*, 263.
31. Kalinin V. N., Usatov A. V., Zakharkin L. I.: *Zh. Obshch. Khim.* **1987**, *57*, 2508.
32. a) Iogansen A. V. in: *Vodorodnaya Svyaz'* (N. D. Sokolov, Ed.). Nauka, Moskva 1981; b) Iogansen A. V: *Spectrochim. Acta, Part A* **1999**, *55*, 1585.
33. Churchill M. R., DeBoer B. G.: *J. Am. Chem. Soc.* **1974**, *96*, 6310.
34. a) Yanovsky A. I., Struchkov Yu. T., Kalinin V. N., Zakharkin L. I.: *Zh. Strukt. Khim.* **1982**, *23*, 77; b) Grushin V. V., Tolstaya T. P., Yanovsky A. I., Struchkov Yu. T.: *Bull. Akad. Sci. U.S.S.R., Div. Chem. Sci.* **1984**, 788; c) Zakharkin L. I., Olshevskaya V. A., Zhigareva G. G., Antonovich V. A., Petrovsky P. V., Yanovsky A. I., Polyakov A. V., Struchkov Yu. T.: *Metallorg. Khim.* **1989**, *2*, 1274.
35. Vinas C., Butler W. M., Teixidor F., Rudolph R. W.: *Inorg. Chem.* **1986**, *25*, 4369.
36. a) Cowie J., Hamilton E. J. M., Laurie J. C. V., Welch A. J.: *Acta Crystallogr., Sect. C: Cryst. Struct. Commun.* **1988**, *44*, 1648; b) Buchanan J., Hamilton E. J. M., Reed D., Welch A. J.: *J. Chem. Soc., Dalton Trans.* **1990**, 677.
37. Copley R. C. B., Mingos D. M. P.: *J. Chem. Soc., Dalton Trans.* **1996**, 491.
38. Chiu K., Zhang Z., Mark T. C. W., Xie Z.: *J. Organomet. Chem.* **2000**, *614–615*, 107.
39. Fanfrlik J., Hnyk D., Lepšik M., Hobza P.: *Phys. Chem. Chem. Phys.* **2007**, *9*, 2085.
40. Knoth W. H.: *J. Am. Chem. Soc.* **1967**, *89*, 1274.
41. Frisch M. J., et al.: *Gaussian-94W*, Revision E.2. Gaussian, Inc., Pittsburgh (PA) 1995.
42. Cheeseman J., Keith T. A., Bader R. W. F.: *AIMpac Program Package*. McMaster University, Hamilton (Ontario), Canada 1992.